

Characterization of H-mode Discharges in NSTX

R. Maingi^a, M.G. Bell^b, R.E. Bell^b, C.E. Bush^a, E.D. Fredrickson^b, D.A. Gates^b, S.M. Kaye^b, H.W. Kugel^b, B.P. LeBlanc^b, J.E. Menard^b, D. Mueller^b, S.A. Sabbagh^c, D. Stutman^d, G. Taylor^b, D.W. Johnson^b, R. Kaita^b, R.J. Maqueda^e, M. Ono^b, F. Paoletti^c, Y-K.M. Peng^a, A.L. Roquemore^b, C.H. Skinner^b, V.A. Soukhanovskii^b, E.J. Synakowski^b

^a*Oak Ridge National Laboratory, Oak Ridge TN, 37831 USA*

^b*Princeton Plasma Physics Laboratory, PO Box 451, Princeton, NJ, 08543 USA*

^c*Columbia University, New York, NY, USA*

^d*Johns Hopkins University, Baltimore, MD, USA*

^e*Los Alamos National Laboratory, Los Alamos, NM, 87545 USA*

We report the observation of the first H-mode transitions in the National Spherical Torus Experiment (NSTX). Energy confinement time transiently increased by more than a factor of 2, to order 100 ms. The heating power requirement for accessing the H-mode regime (power threshold) was significantly higher than predicted by a multi-machine database¹ compiled from conventional aspect ratio tokamaks. Our power threshold results are similar to other STs, such as the START and MAST machines^{2,3}. These H-mode observations in STs challenge and extend the existing international power threshold and energy confinement time scalings⁴ based on conventional aspect ratio tokamaks. The remainder of this paper discusses characteristics of the H-modes in NSTX. Additional details are given in ref. [5].

NSTX is a relatively new fusion research facility^{6,7} ($R=0.86\text{m}$, $a=0.67\text{m}$, $R/a \geq 1.26$, $B_t \leq 0.45\text{ T}$), which commenced physics operation in July 1999. NSTX was designed for operation at 1 MA of plasma current (I_p) but has achieved 1.4 MA. Auxiliary heating systems include a neutral beam injector (NBI), capable of delivering 5 MW to NSTX, and a radio-frequency system designed for 6 MW input power. All of the plasma facing components on the center stack and divertor are clad in graphite armor. NSTX employs a conventional wall conditioning program⁸, which includes center stack resistive bake-out up to 300 deg. C, glow discharge cleaning, and boronization^{9,10}. An overview¹¹ of results is given at this conference.

H-modes in NSTX have characteristics similar to tokamak H-modes. Fig. 1 compares the characteristics of the longest H-mode duration obtained to date in NSTX with an L-mode reference discharge. These discharges had $I_p=1\text{ MA}$ and neutral beam injection power ($P_{\text{NBI}} = 1.5\text{ MW}$) (fig. 1a, 1b). Edge visible light, measured by filtered visible spectroscopy (e.g. D_α in fig. 1c) and a fast visible camera, decreased on a 1 ms time scale at the H-mode transition. This decrease indicated a drop in the scrape-off layer electron density, as often observed during H-mode transitions in tokamaks. While the scrape-off layer density decreased, the electron density (n_e) just inside the magnetic separatrix increased, i.e. a steep edge density gradient was observed. Fig. 2 compares the n_e , electron temperature (T_e), and electron pressure (P_e) profiles from Thomson scattering for the discharges in Fig. 1. The H-mode transition occurred at $t=191\text{ ms}$ in discharge #104312, and evidence of an increase in the edge n_e gradient relative to the L-mode reference was shown by the first Thomson data following the transition at $t=197\text{ ms}$. The n_e profile continued to evolve and actually developed a hump at the edge by $t=230\text{ ms}$ in the H-mode discharge. The T_e profile responded to the improved H-mode confinement on a longer time scale, and evidence of a weak T_e pedestal was observed at $t=230\text{ ms}$ in the H-mode case. The broader n_e and T_e profiles in the H-mode lead to a decrease in the pressure peaking factor ($P_{\text{peak}} \equiv P_0/P_{\text{av}}$, with P_0 =central pressure and P_{av} = volume average pressure) computed with EFIT, from 2.4 in the L-mode down to as low as 2.1. The electron kinetic pressure peaking factor ($P_{\text{peak,e}} \equiv P_{0,e}/P_{\text{av,e}}$, obtained from the raw

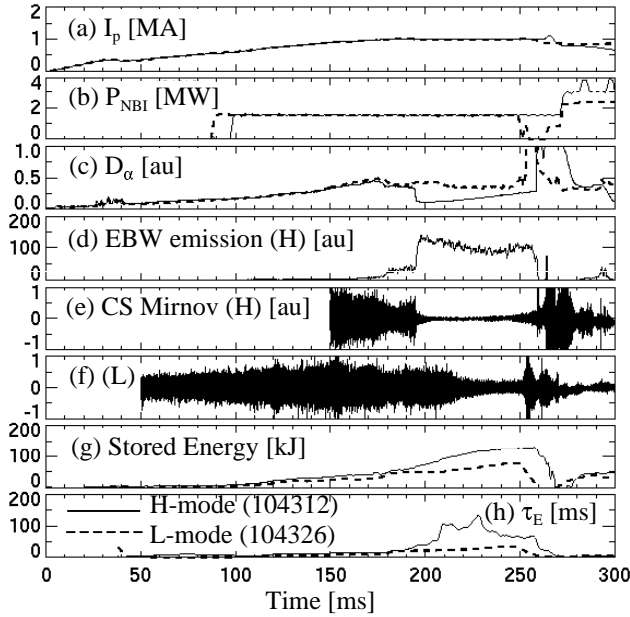


Fig. 1 - Comparison of L-mode (dashed lines in panels) and H-mode (solid lines) discharges in (a) I_p , (b) NBI power, (c) divertor D_α emission, (d) Electron Bernstein Wave (EBW) emission at $R=0.85m$, (e) Center stack Mirnov signal (H-mode), (f) Center stack Mirnov signal (L-mode), (g) stored energy, and (h) τ_E . Panels (g) and (h) are obtained from EFIT reconstruction.

gradually reduced as the plasma X-point was formed at 170 ms in both discharges, but that the H-mode discharge exhibited a rapid drop at the L-H transition. However the fluctuation level in the H-mode discharge began to increase slowly at 245 ms, indicating the onset of new magneto-hydrodynamic (MHD) activity (discussed later).

The peak stored energy, obtained by magnetic equilibrium reconstruction with the EFIT code^{13,14}, was 60% higher in the H-mode phase compared to that of the L-mode reference discharge (fig. 1g). These values correspond to toroidal beta ($\beta_t \equiv 2\mu_0 P_{av}/B_t^2$) of 10% and 6% respectively. The peak rate of rise of both the plasma stored energy, dW/dt , and the plasma electron inventory, dN_e/dt , more than doubled in the H-mode phase, up to 1.7 MW and 2.3×10^{20} electrons/s respectively. The L-mode reference discharge in figs. 1-2 had gas puffing to achieve comparable line-average density prior to the L-H transition in the H-mode discharge. This gas puffing during NBI apparently reduced τ_E to ≤ 35 ms in the reference discharge (fig. 1h). In comparison, lower density L-modes without gas puffing during NBI in NSTX achieved peak $\tau_E \leq 50$ ms and stored energy ~ 100 kJ.

The estimated τ_E during the H-mode phase (fig. 1h) varied between 70 ms and 120 ms, and was up to 3 times higher than the L-mode reference discharge shown. In computing the loss power for the τ_E estimate, the dW/dt term and time derivative of the poloidal field and toroidal field energy were subtracted off, but the core radiation, NBI shine-through and first orbit loss components were not subtracted. In addition, the stored energy computed by EFIT contains the fast ion component. A useful normalization is the confinement time predicted by an international edge localized mode (ELM)-free H-mode scaling⁴, which is based on data from NBI heated, high- β , conventional aspect ratio tokamaks with $(R/a) > 2.5$. The

profiles in Fig. 2) also decreased, from 3.7 in the L-mode reference case to 3.1 in the H-mode discharge at $t=230$ ms, due primarily to the flattening of the n_e profile.

Confirmation of the steepening of the edge density gradient during the H-mode phase came from the prompt enhancement of the electron Bernstein wave (EBW) emission¹² (fig. 1d). Mode conversion of electrostatic electron Bernstein waves to electromagnetic, X-mode radiation becomes more efficient as the edge density gradient increases.

The energy confinement in H-modes in conventional aspect ratio tokamaks increases typically by 60-80% over L-mode levels. This increase in τ_E has previously been correlated with reduced transport at the edge (and sometimes in the core), as manifested in steep edge n_e gradients. The reduced transport is in turn caused by a reduction in the turbulence levels. A signature of the reduced edge turbulence in the NSTX H-modes was observed on the center stack Mirnov signals in fig. 1e. Fig. 1f shows the L-mode reference case. Note that the envelope of the oscillations was

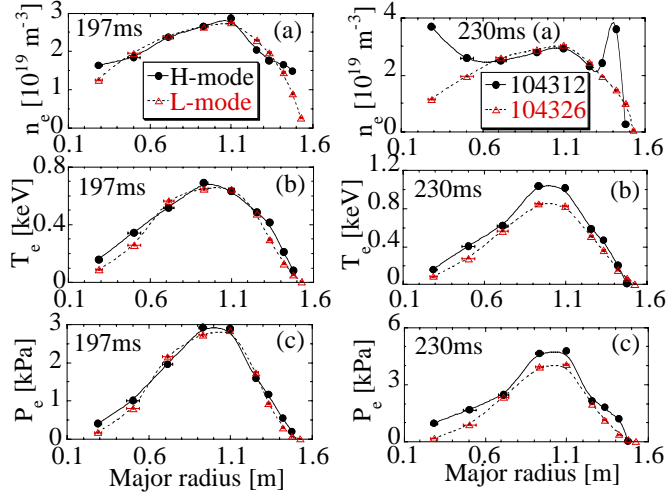


Fig. 2 - Comparison of n_e , T_e , and P_e profiles for L-mode and H-mode (a) 5 ms after time of the H-mode transition, and (b) 33 ms later, during the ELM-free phase. The outer midplane separatrix lies between 1.45 and 1.50m, and the inner midplane separatrix between 0.19 and 0.22m.

ratio. Other diagnostic signatures are discussed in reference [5].

H-mode access for NSTX has been observed in the following range of conditions: $0.7 \leq I_p \leq 1$ MA, $B_t = 0.45$ T, 0.85 MW $\leq P_{\text{NBI}} \leq 1.6$ MW, 0.6 MW $\leq P_{\text{OH}} \leq 1.5$ MW (ohmic heating power), $1.7 \times 10^{19} \leq \bar{n}_e \leq 2.5 \times 10^{19}$ m $^{-3}$, inner-wall gap ≥ 1 -2 cm, and only in lower-single null diverted shape. In this configuration, the ion-grad B drift direction was toward the X-point, and the X-point height was 18 cm. To date, no center-stack limiter H-modes have been observed, despite that most high-power NSTX discharges were conducted in that configuration. Also, no ohmic H-mode discharges were obtained. As in the START device, H-modes were obtained well above the 60 kW power threshold predicted for NSTX from a multi-machine scaling¹. For example, the reference discharge in fig. 1 had loss power ~ 900 kW. In addition, H-modes were observed only after the third boronization. While it is clear that wall conditions affect H-mode access in NSTX, the precise role is not yet quantified.

H-mode duration in NSTX has ranged from 0.5 ms to 65 ms, all shorter than the estimated τ_E which is ~ 100 ms. The first H-modes on NSTX lasted about 8 ms and were terminated by a localized magnetic reconnection at the periphery, as determined by the ultra-soft X-ray (USXR) array¹⁵ data. This MHD event looked very similar to an ELM¹⁶. Low or medium- m precursors were not observed⁵ in the USXR emission, and the MHD activity was generally reduced in the H-mode phase compared with the preceding L-mode phases. ELMs in tokamaks and also in the START device are usually transient outfluxes of particles and energy. Thus, it is unclear why NSTX did not recover an H-mode phase after the ELM-like event.

The ELM-like termination in the short H-modes is contrasted with more global MHD termination in the longer H-mode. This global MHD termination showed a magnetic precursor. For example, the Mirnov activity is observed to increase at $t=245$ ms during the H-mode in fig. 1(e). The USXR raw data showed⁵ a cold, radiative island with poloidal mode number $m=2$ which began to grow at that time. This mode had toroidal mode number $n=1$, determined by a toroidal Mirnov array. The growth of this cold island, coupled with the rapid increase of the edge carbon emission in the USXR band, suggests that impurities accumulated due to the improvement in particle confinement during the H-mode, and induced

confinement time from this scaling is given by $\tau_E^{\text{ELM-free}} = .0314 I_p^{0.94} B_t^{0.27} n^{0.34} P_{\text{loss}}^{-0.68} R^{1.98} \kappa^{0.68} (a/R)^{0.10} M^{0.43}$, where I_p , B_t , n (plasma density), P_{loss} (power through separatrix), R , and M (working gas mass) have units of MA, T, 10^{19} m $^{-3}$, MW, m, atomic mass units respectively, and κ and a/R are dimensionless. The discharge in fig. 1 achieved up to 1.4-2.4 times the 50 ms $\tau_E^{\text{ELM-free}}$ predicted for NSTX parameters. A second commonly-used H-mode scaling IBP98(y,2), based⁴ on ELMy H-mode discharges, predicted a τ_E of ~ 80 ms for NSTX, i.e. actually higher than the ELM-free scaling. The excellent performance of NSTX relative to either of these scalings underscores the significance of achieving H-mode, which will lead to an extension of the databases and scalings to low aspect

a tearing mode due to enhanced radiation near rational mode surfaces, as also observed¹⁷ in ASDEX-Upgrade. In future experiments, impurity accumulation could possibly be eliminated by inducement of regular ELMs, which typically purge the edge plasma of impurities. The fact that these discharges were ELM-free suggests (from tokamak experience) that NSTX was operated close to the L-H power threshold, and that further increase of heating power should induce conventional ELMs. The operational challenge to extend the H-modes is to understand and prevent the ELMs from returning the discharge to L-mode, as well as avoiding any β -related instabilities due to the increase in NBI power used to trigger ELMs.

In summary, we have induced H-mode discharges in NSTX, in which the energy confinement time increased transiently by between 100-200%. These H-modes had energy confinement well above ELM-free H-mode scaling laws, and had a significantly greater threshold power than predicted. Thus H-modes in NSTX will eventually help extend the confinement and threshold power scalings to low aspect ratio. Finally, H-modes have broader pressure profiles than L-modes (e.g. the pressure peaking factor was reduced by ~15% in NSTX), and broad profiles generally have higher β limits in tokamaks due to improved low-n kink stability, e.g. TFTR¹⁸ and DIII-D¹⁹. Thus achievement of H-modes is a potential path for achieving higher β in NSTX.

This research was supported by the U. S. Dept. of Energy under contracts DE-AC05-00OR22725, DE-AC02-76CH03073, W-7405-ENG-36, and grant DE-FG02-99ER54524. We gratefully acknowledge the contribution of the NSTX technical staff and neutral beam operations staff.

References

-
- ¹ J.A. Snipes, in *Proc. of the 24th EPS Conference*, Berchtesgaden, Germany (European Physical Society, Geneva, 1997), Pt. III, p. 961.
 - ² A. Sykes et. al., *Phys. Rev. Lett.* **84**, 495 (2000).
 - ³ A. Sykes et. al., *Phys. Plasmas* **5**, 2101 (2001).
 - ⁴ ITER physics basis authors, *Nucl. Fusion* **39**, 2137 (1999).
 - ⁵ R. Maingi et. al., 'Characteristics of the First H-mode Discharges in NSTX', submitted to *Phys. Rev. Lett.*, 5/01.
 - ⁶ M. Ono et. al., *Phys. Plasmas* **4**, 799 (1997).
 - ⁷ C. Neumeyer et. al., *Fusion Eng. and Design* **54**, 275 (2001).
 - ⁸ H.W. Kugel et. al., *J. Nucl. Mater.* **290-293** 1185 (2001).
 - ⁹ J. Winter, *Plasma Phys. Contr. Fusion Fusion* **36**, B263 (1994).
 - ¹⁰ C.H. Skinner et. al., "Effect of Boronization on Ohmic Plasmas in NSTX", submitted to *Nucl. Fusion*, 4/2001.
 - ¹¹ J. Menard et. al., this conference.
 - ¹² G.Taylor et. al., *Rev. Sci. Instrum.* **72**, 285 (2001)
 - ¹³ L.L. Lao et. al., *Nucl. Fusion* **25**, 1611 (1985).
 - ¹⁴ S.A. Sabbagh et. al., "Equilibrium Properties of Spherical Torus Properties in NSTX", *Nucl. Fusion* in press, 6/01.
 - ¹⁵ D. Stutman et al., *Rev. Sci. Instrum.* **70**, 572(1999).
 - ¹⁶ ASDEX team, *Nucl. Fusion* **29**, 1959 (1989).
 - ¹⁷ W. Suttrop et. al., *Nucl. Fusion* **37**, 119 (1997).
 - ¹⁸ S.A. Sabbagh et. al., *Fusion Energy* 1996, 921 (International Atomic Energy Agency, Vienna 1997).
 - ¹⁹ E. A. Lazarus et. al., *Fusion Energy* 1996, 199 (International Atomic Energy Agency, Vienna 1997).